

Golmohammadi et al, *J Dent Res Dent Clin Dent Prospects*. 2025;19(2):128-136 doi: 10.34172/joddd.025.41796 https://joddd.tbzmed.ac.ir



Original Article



Effect of nanohydrogel-containing Ferula gummosa resin on Streptococcus mutans and Candida albicans

Shima Golmohammadi^{1*}, Behnaz Daraei², Ali Basir³, Marzieh Rashidipour⁴

- ¹Department of Periodontics, Faculty of Dentistry, Lorestan University of Medical Sciences, Khorramabad, Iran
- ²Faculty of Dentistry, Lorestan University of Medical Sciences, Khorramabad, Iran
- ³Department of Prosthodontics, Faculty of Dentistry, Lorestan University of Medical Sciences, Khorramabad, Iran
- ⁴Razi Herbal Medicines Research Center, Lorestan University of Medical Sciences, Khorramabad, Iran

ARTICLE INFO

Article History: Received: September 23, 2024 Revised: May 14, 2025 Accepted: May 16, 2025 ePublished: June 30, 2025

Keywords

Candida albicans, Ferula, Nanoparticles, Plant extracts, Streptococcus mutans

Abstract

Background. Integrating nanoparticles with herbal medicine can enhance drug efficacy and leverage natural antimicrobial properties, addressing concerns related to drug side effects and microbial resistance. *Streptococcus mutans* and *Candida albicans*, key oral pathogens responsible for dental caries and candidiasis, pose significant clinical challenges. This study investigated the potential of *Ferula gummosa*-based nanoparticles in combating the oral pathogens *S. mutans* and *C. albicans*. **Methods.** In this in vitro study, *F. gummosa* essential oil was extracted and analyzed using gas chromatography-mass spectrometry (GC-MS). A nanogel incorporating this oil was formulated with chitosan and tripolyphosphate (TPP). The physicochemical properties of the nanogel were characterized using scanning electron microscopy (SEM), Fourier transform infrared spectroscopy (FTIR), zeta potential analysis, dynamic light scattering (DLS), and atomic force microscopy (AFM). The minimum inhibitory concentration (MIC), minimum bactericidal concentration (MBC) against *S. mutans*, and minimum fungicidal concentration (MFC) against *C. albicans* were determined through microdilution assays.

Results. The major constituents of *F. gummosa* essential oil were identified as γ-cadinene (20.44%), T-cadinol (12.03%), sabinene (10.23%), and β-pinene (9.77%). The nanogel demonstrated efficient oil encapsulation, with an average nanoparticle size of 128.89 ± 24.08 nm and a PDI of 0.226. The zeta potential of the nanoparticles increased upon oil incorporation. The MIC against *S. mutans* was 19.02 µg/mL for the nanogel and 781.25 µg/mL for the oil, while the MIC against *C. albicans* was 2.37 µg/mL for the nanogel and 195.31 µg/mL for the oil. MBC and MFC assays confirmed the enhanced antimicrobial efficacy of the nanogel.

Conclusion. *F. gummosa* essential oil exhibited significant antibacterial and antifungal properties. Formulating the oil into a nanostructure significantly enhanced its efficacy against *S. mutans* and *C. albicans*, presenting a promising alternative antimicrobial strategy.

Introduction

The growing interest in traditional "green medicine" is driven by concerns about the cost and side effects of synthetic drugs and the escalating resistance of pathogens to standard antibiotics.1 This has reignited enthusiasm for traditional medicinal plants, globally acknowledged for their therapeutic value.² One such plant, Ferula gummosa, indigenous to Iran, is reputed for its anti-inflammatory and antioxidant effects.3 The proven efficacy of its root resin against certain bacteria and fungi further underscores its medicinal potential.^{4,5} Historically, F. gummosa has served various purposes, including traditional applications as an antiseptic, anti-seizure agent, anti-spasm remedy, pain reliever, inflammation reducer, and a tonic for memory enhancement. Recent investigations have substantiated its diverse therapeutic applications, including antimicrobial, anti-inflammatory, antinociceptive,

spasmolytic properties.6

Dental caries, a prevalent infectious oral disease, is closely associated with the formation of dental plaque biofilms.⁷ During the initial stages of dental caries development, the collaborative activity of enzymes (glucosyltransferase and fructosyltransferase) released by Streptococcus mutans, a key cariogenic bacteria, and adhesive-enhancing agents (glucans) secreted by Candida albicans creates environments conducive to the proliferation of other causative bacteria.8 C. albicans, in addition to its role in dental caries, is the microorganism responsible for oral candidiasis, the most prominent fungal disease of the oral cavity.9 Challenges, including resistance to antifungal treatments and side effects, have prompted researchers to explore new antifungal agents, especially those derived from natural compounds. Moreover, most oral diseases, including dental caries and

^{*}Corresponding author: Shima Golmohammadi, Email: shimag221@gmail.com

periodontal diseases, result from biofilms whose structure shields pathogenic bacteria from antibiotics, posing a significant challenge to effectively controlling oral microorganisms. Traditional antimicrobial agents like chlorhexidine gluconate, used to minimize and prevent biofilm formation, come with drawbacks, including dark stains on teeth, alterations in oral microbiota, a burning sensation in the mouth, enhanced calculus formation, and changes in taste perception. Consequently, the intensified search for alternative solutions has led to herbal remedies and natural nanoparticles emerging as promising options for combating oral pathogens.

The defensive barrier role of biofilm against conventional antimicrobial agents has led to the proposal of nanotechnology as an innovative strategy against microberelated oral diseases. Nanoparticles' unique physical and chemical characteristics, such as significantly small size and increased surface-to-mass ratio, enhance their antimicrobial properties. 10 Nanomedicine is an innovative approach to enhance the efficiency of herbal constructs.¹¹ The use of natural biopolymers like chitosan as drug carriers in nanoparticles proves effective in harnessing the medicinal properties of plants, offering advantages such as biodegradability, biocompatibility, low toxicity, and enhanced safety.¹² Additionally, the incorporation of natural antimicrobial agents into chitosan amplifies its antimicrobial properties, substantially improving the targeted delivery of therapeutic molecules to cells and tissues. This approach enables a slow and sustained release, optimizing overall effectiveness.13

Due to the multi-faceted therapeutic properties of F. gummosa, it has attracted attention as a promising candidate for controlling oral pathogens.¹⁴ While studies have investigated the effects of F. gummosa resin on various microorganisms,5,15 none have applied nanotechnology to improve the bioavailability and efficacy of the essential oil derived from various parts of the plant. This study explored the potential of nanohydrogel-containing F. gummosa resin as a natural therapeutic agent against two major dental pathogens, S. mutans and C. albicans.

Methods

Plant preparation and oleo-resin extraction

Ferula gummosa was initially obtained from a local herbal market. It was then identified by a herbarium center at a university, and the voucher herbarium code PMP-1859 was assigned. The resin was collected by making incisions on the rhizome or upper roots of the plant and stored in a dry, shaded environment away from direct sunlight. Additionally, to increase the contact surface and reduce its volume, the obtained resin was dried and finely ground using a grinder.

Essential oil

Ferula gummosa essential oil was obtained using the distillation method. In this process, 100 grams of F. gummosa resin were immersed in one liter of distilled

water and subjected to hydro-distillation within the Clevenger apparatus for 3 hours. Subsequently, the resulting essential oil was stored at 4 °C until the following experimental stages.

Gas chromatography-mass spectrometry analysis (GC-MS)

GC-MS analysis was conducted using an AGILENT 7890A gas chromatograph combined with a mass spectrometer (Model 5975C, Agilent Technologies, Santa Clara, CA, USA) to analyze volatile and semi-volatile compounds within the essential oil. A GC capillary column, SGE-BP20 (composed of phenyl methyl siloxane with a length of 30 meters, an internal diameter of 250 µm, and a film thickness of 0.25 µm, Agilent Technologies), was employed. The oven temperature was programmed to increase from 60 °C to 230 °Cat a rate of 8 °C/min. The injection port temperature was held at 280 °C, and helium gas served as the carrier gas with a flow rate of 1.3 mL/ min. Mass spectrometry was performed using electron ionization at an energy level of 70 eV within a mass range of 20-550 Da. The constituents of the F. gummosa essential oil were identified by comparing their Kováts retention indices (KI) and mass spectra with known compounds available in the NIST 2014 library.¹⁶

Nanohydrogel preparation

The research aimed to encapsulate F. gummosa resin oil within chitosan nanoparticles (CSNPs) and used tripolyphosphate (TPP) as a cross-linking agent to fabricate F. gummosa resin oil-loaded CSNPs. Separate solutions of 0.5% chitosan and 0.3% TPP were meticulously prepared for the experiment. Initially, 0.1 grams of low molecular weight chitosan was gradually introduced into 20 mL of a 1% acetic acid solution while continuously stirring for 2 hours. Subsequently, 5 mL of Tween 20 emulsifier was incorporated, and the mixture was stirred for an additional 2 hours. Following this, 1 mL of F. gummosa resin oil was introduced slowly and drop by drop over 20 minutes into the chitosan acidic solution while ensuring continuous stirring. Finally, 5 mL of an 0.3% TPP solution was added to induce the formation of a hydrogel network. This particular hydrogel, characterized by its nano-sized cavities, was achieved through ionotropic gelation. Highspeed centrifugation was then executed to separate the supernatant solution containing the nanohydrogel from the sedimented phase.

In a parallel experiment, a blank nanohydrogel, i.e., without including F. gummosa resin oil, was synthesized using identical procedures and proportions as outlined above.

Tests performed on nanohydrogel UV-vis spectrophotometry

The encapsulation efficiency of F. gummosa in the nanohydrogel was assessed using UV-Vis spectroscopy with a UV-Vis spectrophotometer (UV-1900, Shimadzu,

Kyoto, Japan). This instrument uses lamps emitting light in the visible (tungsten lamp) and UV (deuterium lamp) regions, covering wavelengths from 190 nm to 900 nm. It enables the analysis of samples based on their lightabsorbing properties. The maximum wavelength of light absorption (λmax) for *F. gummosa* resin oil was determined, and subsequently, the optical density (OD) at this specific wavelength was measured for various concentrations of F. gummosa resin oil and nanohydrogel containing the resin oil. These OD values were used to construct a calibration curve, facilitating precise quantification of F. gummosa resin oil concentration within the nanohydrogel.

Encapsulation efficiency=(mass of loaded F. gummosa/ mass of initial F. gummosa) × 100

Scanning electron microscopy (SEM)

The morphology of the synthesized nanoparticles was studied using SEM. Freeze-dried nanoparticles were positioned on a gold-coated stub and examined at 15 kV with a 6300-field emission scanning electron microscope (Hitachi, S-4160).

Zeta potential and dynamic light scattering (DLS) analysis

Zeta potential analysis was employed to determine the electric charge of the particles using a Malvern Zetasizer Nano-range instrument (Malvern Instruments Ltd., Malvern, UK). Additionally, DLS analysis was performed to measure particle sizes, which involved observing laser light interactions with the particles, recording scattering patterns, and capturing variations in light intensity due to the Brownian motion of the particles.

Fourier transform infrared spectroscopy (FTIR)

FTIR spectroscopy was conducted to identify functional groups and elucidate the structure of the organic compounds. IR light was directed at the three test materials: F. gummosa resin essential oil, nanohydrogel containing F. gummosa resin oil, and the blank nanohydrogel (comprising chitosan and TPP). Functional groups were identified based on the absorption or transmission of IR radiation using the BRUKER TENSOR 27 instrument (Germany).

Atomic force microscopy (AFM)

AFM was used to analyze the surface topography of the samples. Using electrostatic interactions between the atoms at the tip and those on the sample surface, the tip exhibited upward and downward deflections. These deflections were detected by a laser and photodiode integrated into the microscope, facilitating the creation of three-dimensional images of the samples at nanoscale dimensions. AFM analysis was performed on 200 microliters of nanohydrogels containing F. gummosa resin oil and blank nanohydrogels, deposited on a glass slide, and examined after air-drying at room temperature, using the AFM instrument model of 0101/A (Ara Research Co Nano Experts, Iran).

Microbial and fungal specimens

The selected standard strains of S. mutans (ATCC35668) and C. albicans (ATCC10231) were purchased from the National Center for Genetic and Biological Resources of Iran.

Minimum inhibitory concentration (MIC) and minimum bactericidal concentration (MBC)

The MIC and MBC for S. mutans and the MIC and MFC for C. albicans were determined using the microdilution method in sterile 96-well plates, following the protocol established by the Clinical and Laboratory Standards Institute (CLSI).17

Initially, stock solutions for the three study groups were prepared, including F. gummosa essential oil, nanohydrogel containing F. gummosa essential oil, and blank nanohydrogel. A sterile culture medium was also prepared, employing brain-heart infusion (BHI) for S. mutans and Sabouraud dextrose broth for C. albicans. The stock solution of F. gummosa essential oil was set at a concentration of 200 000 µg/mL. In comparison, the stock solutions of the nanohydrogel were prepared at a concentration of 120 000 µg/mL, based on the total weight of the nanohydrogels.

Subsequently, 100 µL of the sterile culture medium was added to rows three through twelve of the 96-well plates. In the first two rows, $100 \mu L$ was introduced from the prepared bacterial inoculum, initiating a serial dilution process from the second to the tenth row. This dilution involved transferring 100 µL from the second row to the third row and 50 µL from the third row to the fourth through the tenth row. In rows two to ten, 10 µL of a 24-hour microbial culture, equivalent to 0.5 McFarland turbidity $(1.5 \times 10^8 \text{ CFU/mL})$, was added.

The antimicrobial effect of F. gummosa essential oil was evaluated in the 96-well plates at concentrations of 100,000 μ g/mL for the essential oil and 60 000 μ g/mL for the nanohydrogels. These plates were then incubated for 24 hours at 37 °C.

Following incubation, 2,3,5-triphenyl tetrazolium chloride (TTC) was used as a visual indicator for bacterial growth. Wells that exhibited no change in color were designated as the MIC. Colorless wells were subjected to sub-culturing on Mueller-Hinton agar medium for S. mutans and Sabouraud dextrose agar for C. albicans to determine the MBC and MFC, respectively. The negative control consisted of dimethyl sulfoxide (DMSO), while 0.2% chlorhexidine (CHX) was used as the positive control for S. mutans, and 100 000-IU/mL nystatin served as the positive control for *C. albicans*.

Data analysis

All measurements were conducted three times. One-way analysis of variance (ANOVA) in SPSS 23 (SPSS Inc., Chicago, IL, USA) was used to determine the statistical

significance of the experimental results. In the cell viability test, significance was attributed to *P* values < 0.05.

Results

Table 1 summarizes the essential oil constituents and their respective percentages. The viscosity, dielectric constant, and zeta potential of the F. gummosa nanohydrogel were compared to those of the blank nanohydrogel, as summarized in Table 2.

The maximum light absorption (λ max) of the F. gummosa essential oil was observed at a wavelength of 259 nm. Using UV-Vis spectrophotometry, a calibration curve was generated from OD measurements at five different

Table 1. Chemical components (%) of F. gummosa essential oil was analyzed

No.	Compound	Retention time (min)	Content (%)
1	α-Pinene	1.43	3.23
2	β-Pinene	1.51	9.77
3	Sabinene	1.6	10.23
4	o-Cymene	2.86	1.94
5	α-Copaene	5.72	5.7
6	Germacren D	6.44	0.63
7	Pinocarvone	6.78	1.39
8	Aromandendrene	7.31	2.39
9	Terpinen-4-ol	7.56	7.56
10	cis-Muurola-4(15),5- diene	8.8	8.8
11	Epizonarene	9.83	1.07
12	α-Muurolene	10.161	1.48
13	γ-Cadinene	10.95	20.44
14	Unknown	16.42	5.9
15	Epicubenol	18.39	1.34
16	Guaiol	19.06	1.53
17	T-Cadinol	20.22	12.03
18	Bulnesol	20.78	1.86
19	α-Cadinol	21.03	0.62
Total	identified		92.91

essential oil concentrations. After determining the OD of a specific concentration of the nanohydrogel containing F. gummosa resin essential oil, the concentration of resin essential oil within the nanohydrogel was quantified using the derived formula (y = 0.0022x + 0.0288). The OD of F. gummosa resin essential oil at a concentration of 50.000 μg/mL yielded a measurement of 0.168. Substituting this value into the formula (in place of 'y') allowed calculating the resin essential oil concentration in the nanohydrogel, resulting in 43.63 µg/mL. These calculations revealed that the concentration of F. gummosa essential oil in the stock solution, prepared for the evaluation of its antimicrobial properties, was determined to be 2.152 µg/mL (equivalent to 0.6 grams of the nanohydrogel containing F. gummosa essential oil dissolved in 5 mL of distilled water). Figure 1 illustrates the calibration curve based on the absorbance of F. gummosa essential oil at varying concentrations.

SEM and AFM views of the blank nanohydrogel and the nanohydrogel loaded with F. gummosa resin oil are depicted in Figures 2 and 3.

The DLS data, as depicted in Figure 4, indicated that the average particle size (Z-ave) within the F. gummosa resin oil-containing nanohydrogel was measured at 128.89 ± 24.8. Furthermore, the polydispersity index (PDI) for the nanohydrogel containing F. gummosa resin oil was reported as 0.226, while the blank nanohydrogel exhibited a PDI of 0.792.

Figure 5 exhibits the FTIR spectra of blank nanohydrogel, the nanohydrogel loaded with F. gummosa and F. gummosa essential oil, emphasizing their distinct infrared transmittance spectral patterns.

Tables 3 and 4 present the MIC and MBC of F. gummosa

Table 2. Viscosity, dielectric constant, and zeta mean comparison between blank nanohydrogel and F. gummosa nanohydrogel

Parameter	Blank nanohydrogel	F. gummosa nanohydrogel
Viscosity	0.9307 MPa	0.9472 MPa
Dielectric constant	79.10	79.37
Zeta mean	0.04 ± 1.70 mV	-7.38±9.57 mV

Table 3. MIC and MBC against Streptococcus mutans for study groups and controls

Group	MIC (µg/mL)	95% CI (MIC)	P-value (MIC)	MBC (µg/mL)	95% CI (MBC)	P value (MBC)
Blank nanohydrogel	30000	28500-31500		60000	57000-63000	
F. gummosa nanohydrogel	19.02	18.1–20.0		19.02	18.4–19.6	
F. gummosa essential oil	781.25	740-823	0.0013	781.25	750-812	0.0011
CHX	0.98	0.93-1.03		1.96	1.85-2.07	
DMSO	Growth in all concentrations	-		-	-	

Table 4. MIC and MFC against Candida albicans for study groups and controls

	MIC (μg/mL)	95% CI (MIC)	P value (MIC)	MFC (µg/mL)	95% CI (MFC)	P value (MFC)
Blank nanohydrogel	3750	3575–3925		7500	7150–7850	
F. gummosa nanohydrogel	2.37	2.25-2.50		4.75	4.50-5.00	
F. gummosa essential oil	195.31	185–206	0.0027	195.31	185–206	0.0021
Nystatin	1.22	1.15–1.29		1.22	1.15–1.29	
DMSO	Growth in all concentrations	-		-	-	

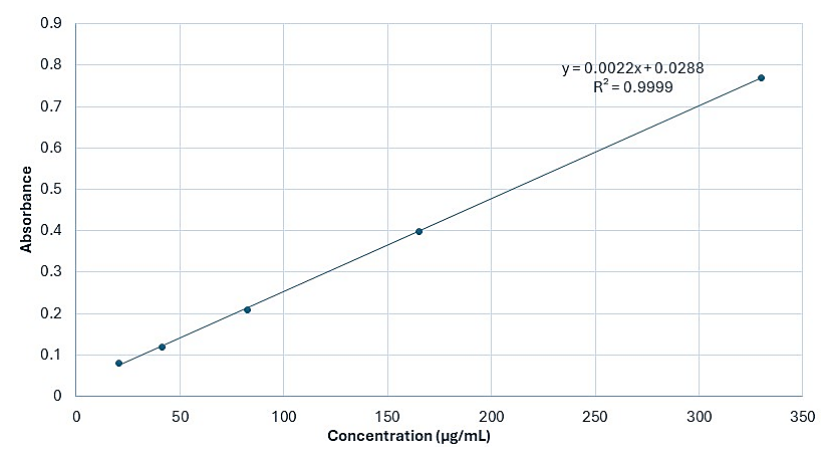
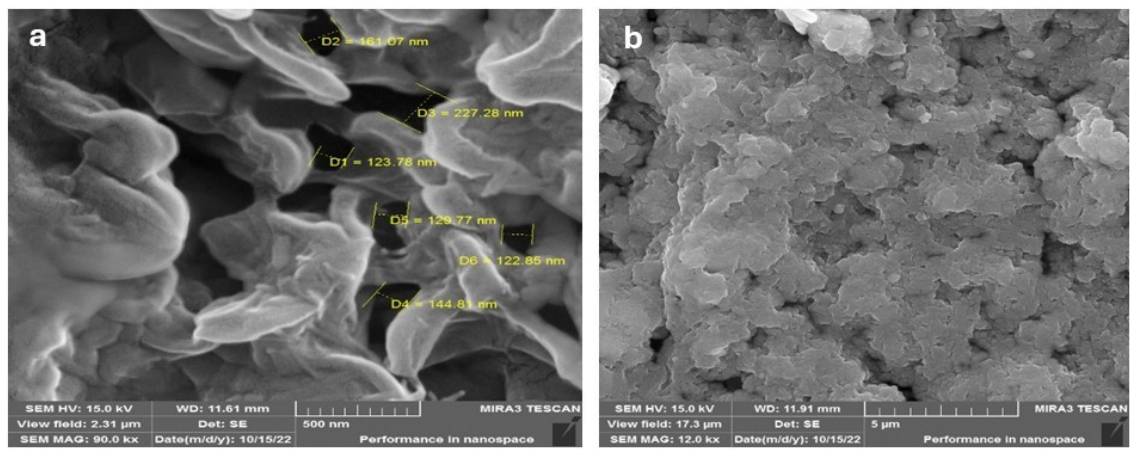


Figure 1. Calibration curve of F. gummosa essential oil absorbance at varying concentrations ($\lambda_{ax} = 259$ nm), using UV-Vis spectrophotometry to quantify essential oil in the nanohydrogel formulation



 $\textbf{Figure 2.} \ \textbf{SEM images of (a) blank nanohydrogel at } 90\,000 \times \textbf{and (b) nanohydrogel loaded with } \textit{F. gummosa essential oil at } 12\,000 \times \textbf{magnification.} \ \textbf{The loaded } \textbf{SEM images of (a) blank nanohydrogel at } \textbf{SEM images of$ formulation shows a denser, more compact surface, indicating successful oil encapsulation (scale bars: 500 nm (a), 5 µm (b))

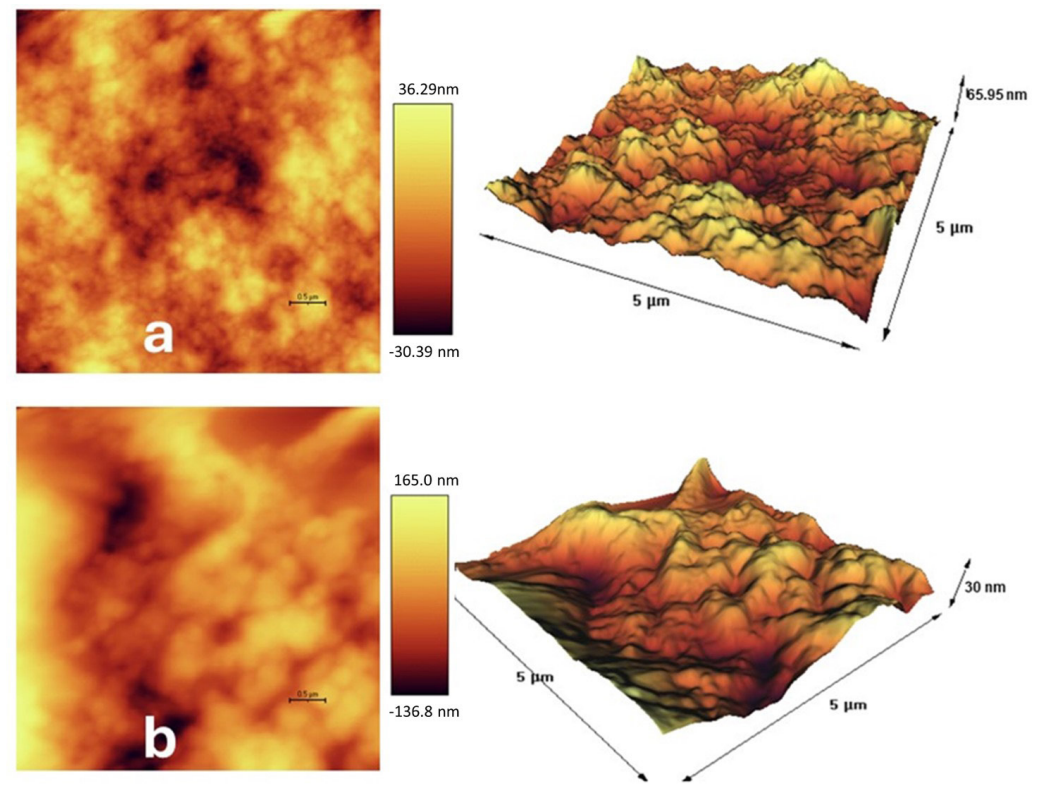


Figure 3. AFM surface topography of (a) blank nanohydrogel and (b) nanohydrogel loaded with F. gummosa essential oil. Increased surface roughness in (b) may $contribute \ to \ enhanced \ antimicrobial \ interaction \ with \ microbial \ membranes. \ (scale \ bars = 0.5 \ \mu m \ (2D \ images) \ and \ 5 \ \mu m \ (3D \ images))$

resin essential oil, nanohydrogels, and positive and negative control substances against *S. mutans*, respectively.

DMSO and nystatin served as negative and positive controls, respectively. Subsequently, the contents of the wells without growth in the MIC test were cultured on a solid Mueller-Hinton agar medium. After 24 hours of anaerobic incubation, the MBC results were examined. The MIC of nystatin against *C. albicans*, determined by microdilution, was 22.1 $\mu g/mL$. Considering that the concentration of nystatin is 100 000 IU/mL, and according to the International Units converter, each IU of nystatin is equivalent to 0.2 μg , the nystatin concentration is 20 000 $\mu g/mL$. Since this concentration was halved with an equal volume of the culture medium, the examination of nystatin concentrations began at 10 000 $\mu g/mL$.

Discussion

Our investigation into the essential oil of *F. gummosa* resin, using GC-MS, revealed a robust composition with notable components, including γ -cadinene, T-cadinol, sabinene, and β -pinene. These constituents, recognized for their antimicrobial properties, have been extensively

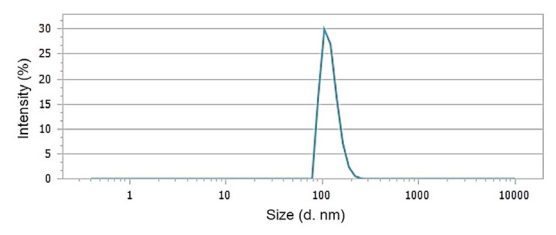


Figure 4. Dynamic light scattering (DLS) analysis of *F. gummosa* nanohydrogel showing an average particle size of 128.89±24.8 nm and a PDI of 0.226, indicating monodisperse nanoparticle distribution suitable for improved bioavailability and interaction with microbial cells

studied for their efficacy against common oral pathogens, including *S. mutans* and *C. albicans*. ¹⁸⁻²³ This study focused on harnessing these properties by developing a nanohydrogel incorporating *F. gummosa* resin essential oil, with a specific emphasis on its potential impact on antimicrobial properties.

The microscopic analysis illustrated nanoscalesized voids in the blank nanohydrogel formed due to electrostatic interactions. These voids were filled after adding *F. gummosa* resin essential oil, resulting in a compact structure.

The zeta potential of the nanohydrogel containing E gummosa resin essential oil was -7.38 mV, indicating improved particle dispersion and stability compared to the blank nanohydrogel (-0.04 mV). DLS revealed an average particle size (Z-ave) of approximately 128.89 \pm 24.8 nm for the nanohydrogel containing E gummosa resin essential oil. The PDI was measured at 0.226, indicating reduced particle aggregation. In contrast, the blank nanohydrogel had a PDI of 0.792, suggesting increased particle aggregation.

Further characterization through FTIR spectra confirmed the successful encapsulation of *F. gummosa* resin essential oil within the nanohydrogel, with specific functional groups corresponding to essential oil peaks not visible.

Three-dimensional AFM images showed a textured surface with varying elevations in the nanohydrogel containing *F. gummosa* resin essential oil. This surface roughness may enhance adhesion to bacteria associated with dental decay, such as *S. mutans*.

Our study unequivocally demonstrated the potent bacteriostatic and bactericidal properties of *F. gummosa*

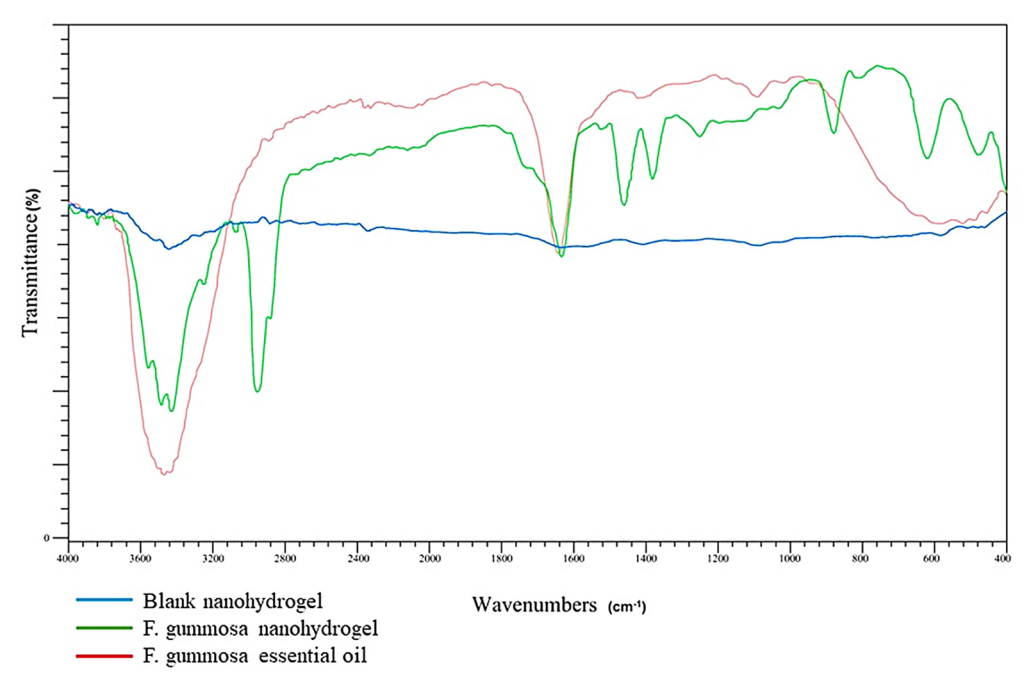


Figure 5. FTIR spectra comparing blank nanohydrogel, *F. gummosa* nanohydrogel, and *F. gummosa* essential oil. Shifts and overlaps in characteristic peaks (e.g., -OH, C=O, C-O-C) indicate the successful incorporation of the oil into the nanohydrogel matrix and suggest interactions involved in encapsulation at the molecular level

resin essential oil against S. mutans. Additionally, the essential oil displayed notable antifungal properties against C. albicans. The integration of the essential oil into a nanogel formulation significantly enhanced its antimicrobial effectiveness, as evidenced by reduced MIC and MBC values compared to the blank nanogel. Comparing our findings with Abbaszadegan et al,5 we observed consistent antibacterial activity against various oral pathogens, including C. albicans, with an MIC against C. albicans reported as 50 µg/mL. Variations in antimicrobial properties between studies underscored the diversity of active compounds in plants from different regions. Furthermore, compared to other studies exploring chitosan and chitosan-based nanoparticles, our study's effectiveness against S. mutans and C. albicans suggested a promising alternative with lower concentrations required for efficacy.

Recent findings in nanotechnology-based phytochemical delivery further support our results. For instance, albumin nanoparticles loaded with Mentha extract exhibited enhanced antibacterial activity against methicillin-resistant Staphylococcus aureus (MRSA) compared to the free extract while maintaining lower cytotoxicity.²⁴ Similarly, silver nanoparticles biosynthesized using Musa paradisiaca (banana) and Citrus sinensis (orange) peel extracts showed strong antimicrobial effects against multidrug-resistant strains such as Acinetobacter baumannii and Klebsiella pneumoniae.25 These examples underscore the role of nanocarrier systems in improving the performance of natural compounds by enhancing their bioavailability, stability, and cellular delivery. Consistent with these findings, our study demonstrated that incorporating F. gummosa essential oil into a nanohydrogel formulation significantly enhanced its antimicrobial efficacy against S. mutans and C. albicans. Unlike studies comparing different plant species, we focused on various formulations of F. gummosa to control for interspecies variability and isolate the effect of nanoencapsulation.

The findings of the present study unequivocally demonstrated the bacteriostatic and bactericidal properties of F. gummosa resin essential oil against S. mutans. Furthermore, the F. gummosa resin essential oil exhibited notable antifungal properties against *C. albicans*. Importantly, integrating F. gummosa resin essential oil into a nanogel formulation significantly amplified its antimicrobial effectiveness against these oral pathogens. This enhancement is evident in the reduced MIC and MBC values, measuring 19.02 µg/mL for S. mutans and 2.37 µg/mL and 4.75 µg/mL for C. albicans, respectively. While chitosan itself demonstrates efficacy against oral microorganisms,^{26,27} it is essential to highlight that the blank nanogel displayed inhibitory and bactericidal effects, albeit at significantly higher concentrations against these pathogens.

Various studies have highlighted the diverse applications of F. gummosa, including its antibacterial properties, incorporation into liposomes, and the synthesis of nanocrystals with potential applications in bioimaging. Our research stands out by focusing on loading F. gummosa resin essential oil onto nanoparticles and investigating their specific effects on S. mutans and C. albicans.

Sepahi et al²⁸ explored the antibacterial and nonhemolytic properties of aqueous extracts derived from F. gummosa against Staphylococcus aureus and Escherichia coli. They reported significant antibacterial effects, with MIC values below 750 µg/mL and no notable hemolytic activity. Notably, unlike our study, Sepahi et al did not specify the plant part used. Nazemisalman et al²⁹ reported that F. gummosa essential oil possesses antibacterial efficacy against Enterococcus faecalis, comparable to CHX, indicating its potential for clinical use in addressing oral and dental pathogens.

Several studies have explored diverse applications of F. gummosa, showcasing its versatility and potential in various fields. Najafi et al.30 loaded liposomes with F. gummosa essential oil, emphasizing heightened antibacterial activity against E. coli, particularly at subinhibitory concentrations. This work aligns with the investigation by Kamelnia et al,31 who produced cellulose nanocrystals from F. gummosa, demonstrating no cytotoxic effects on A549 cells and stability in radiolabeling (Tc-99m), underscoring the potential of F. gummosa-derived materials in bioimaging applications.

In a cytotoxicity context, Mousavi-Kouhi et al32 synthesized gold-coated nanoceria (Au/nanoceria) using F. gummosa gum as a capping agent. The study highlighted a notable toxicological impact on breast cancer cell lines (MCF7) with minimal effects on normal cells, emphasizing the dose and time-dependent nature of nanoceria toxicity. Similarly, Hosseini et al³³ reported cytotoxic and apoptotic effects of F. gummosa gum extract on renal cell carcinoma cell line (ACHN). Forouzmand et al³⁴ also demonstrated that F. gummosa enhanced cytotoxicity in HeLa cells through apoptosis induction and, when co-administered with radiotherapy, significantly increased radiosensitivity, suggesting its potential as a valuable radiosensitizer agent for cervical cancer treatment.

For diabetic control, F. gummosa essential oil-loaded nano-fibers exhibit inhibitory effects on α-amylase and a-glucosidase, maintaining the herb's antioxidant activity.35 Additionally, administering the ethanolic extract of F. gummosa oleo-resin to diabetic rats36 yields antihyperglycemic effects, including reduced fasting blood glucose levels, alleviation of oxidative stressinduced damage in the liver and kidneys, and restoration of antioxidant enzyme activity.

While our findings are promising, additional research is recommended to evaluate the efficacy of F. gummosa resin essential oil and its nanogels against a broader spectrum of oral pathogens. Furthermore, assessing cellular toxicity associated with the essential oil and corresponding nanogels is crucial for a comprehensive understanding. Future studies should explore the effectiveness of essential oil and its nanogel formulation through animal studies or clinical trials.

Conclusion

Ferula gummosa resin essential oil demonstrated promising antimicrobial characteristics, encompassing both bacteriostatic and bactericidal effects. Due to these valuable attributes, it emerges as a potential natural remedy for infectious oral diseases linked to *S. mutans*, including dental caries and those associated with *C. albicans*, specifically various forms of oral candidiasis. The transformation of this essential oil into nanogel form holds the promise of substantially augmenting its antimicrobial efficacy against the diseases mentioned above.

Acknowledgments

The authors have no acknowledgments to declare.

Authors' Contribution

Conceptualization: Shima Golmohammadi.

Data curation: Behnaz Daraei, Ali Basir, Marzieh Rashidipour. Formal analysis: Behnaz Daraei, Ali Basir, Marzieh Rashidipour. Investigation: Behnaz Daraei, Ali Basir, Marzieh Rashidipour.

Methodology: Shima Golmohammadi. **Project administration:** Shima Golmohammadi.

Resources: Behnaz Daraei, Ali Basir, Marzieh Rashidipour.

Supervision: Shima Golmohammadi. **Validation:** Shima Golmohammadi. **Visualization:** Marzieh Rashidipour.

Writing-original draft: Shima Golmohammadi.

Writing–review & editing: Shima Golmohammadi, Behnaz Daraei, Ali Basir, Marzieh Rashidipour.

Competing Interests

None declared.

Ethical Approval

"Consent to Participate" was not applicable as it is an in vitro study conducted in a laboratory setting. The ethics code is IR.LUMS. REC.1401.071.

Funding

The study was funded by the authors, with no external sources of funding.

References

- Nagarajappa S, Bathija P, Mishra P, Bansal V, Gupta S, Sontakke S. Antibacterial and antifungal activity of neem and clove extract against *S. mutans* and *C. albicans*-an invitro study. World J Pharm Res. 2018;7(5):1484-93. doi: 10.20959/ wjpr20185-10806.
- Anand U, Jacobo-Herrera N, Altemimi A, Lakhssassi N. A comprehensive review on medicinal plants as antimicrobial therapeutics: potential avenues of biocompatible drug discovery. Metabolites. 2019;9(11):258. doi: 10.3390/ metabo9110258.
- Moosavi SJ, Habibian M, Peeri M, Azarbayjani MA, Nabavi SM, Nabavi SF, et al. Protective effect of *Ferula gummosa* hydroalcoholic extract against nitric oxide deficiency-induced oxidative stress and inflammation in rats renal tissues. Clin Exp Hypertens. 2015;37(2):136-41. doi: 10.3109/10641963.2014.913609.
- Farid Afshar F, Saffarian P, Mahmoodzadeh Hosseini H, Sattarian F, Amin M, Imani Fooladi AA. Antimicrobial effects of *Ferula gummosa* Boiss gum against extended-spectrum β-lactamase producing *Acinetobacter* clinical isolates. Iran J

- Microbiol. 2016;8(4):263-73.
- Abbaszadegan A, Gholami A, Mirhadi H, Saliminasab M, Kazemi A, Moein MR. Antimicrobial and cytotoxic activity of *Ferula gummosa* plant essential oil compared to NaOCl and CHX: a preliminary in vitro study. Restor Dent Endod. 2015;40(1):50-7. doi: 10.5395/rde.2015.40.1.50.
- Mahboubi M. Ferula gummosa, a traditional medicine with novel applications. J Diet Suppl. 2016;13(6):700-18. doi: 10.3109/19390211.2016.1157715.
- 7. Gao Z, Chen X, Wang C, Song J, Xu J, Liu X, et al. New strategies and mechanisms for targeting *Streptococcus mutans* biofilm formation to prevent dental caries: a review. Microbiol Res. 2023;278:127526. doi: 10.1016/j.micres.2023.127526.
- Falsetta ML, Klein MI, Colonne PM, Scott-Anne K, Gregoire S, Pai CH, et al. Symbiotic relationship between *Streptococcus mutans* and *Candida albicans* synergizes virulence of plaque biofilms in vivo. Infect Immun. 2014;82(5):1968-81. doi: 10.1128/iai.00087-14.
- Patel M. Oral cavity and *Candida albicans*: colonisation to the development of infection. Pathogens. 2022;11(3):335. doi: 10.3390/pathogens11030335.
- Fernandes GL, Delbem ACB, do Amaral JG, Gorup LF, Fernandes RA, de Souza Neto FN, et al. Nanosynthesis of silver-calcium glycerophosphate: promising association against oral pathogens. Antibiotics (Basel). 2018;7(3):52. doi: 10.3390/antibiotics7030052.
- Zhang J, Hu K, Di L, Wang P, Liu Z, Zhang J, et al. Traditional herbal medicine and nanomedicine: converging disciplines to improve therapeutic efficacy and human health. Adv Drug Deliv Rev. 2021;178:113964. doi: 10.1016/j. addr.2021.113964.
- Ashrafi B, Rashidipour M, Marzban A, Soroush S, Azadpour M, Delfani S, et al. *Mentha piperita* essential oils loaded in a chitosan nanogel with inhibitory effect on biofilm formation against *S. mutans* on the dental surface. Carbohydr Polym. 2019;212:142-9. doi: 10.1016/j.carbpol.2019.02.018.
- Rashki S, Asgarpour K, Tarrahimofrad H, Hashemipour M, Ebrahimi MS, Fathizadeh H, et al. Chitosan-based nanoparticles against bacterial infections. Carbohydr Polym. 2021;251:117108. doi: 10.1016/j.carbpol.2020.117108.
- Boghrati Z, Iranshahi M. Ferula species: a rich source of antimicrobial compounds. J Herb Med. 2019;16:100244. doi: 10.1016/j.hermed.2018.10.009.
- Daneshkazemi A, Zandi H, Davari A, Vakili M, Emtiazi M, Lotfi R, et al. Antimicrobial activity of the essential oil obtained from the seed and oleo-gum-resin of *Ferula assa-foetida* against oral pathogens. Front Dent. 2019;16(2):113-20. doi: 10.18502/fid.v16i2.1362.
- National Institute of Standards and Technology. EPA/NIH mass spectral library. Gaithersburg: NIST; 2014.
- Weinstein MP, Lewis JS 2nd. The clinical and laboratory standards institute subcommittee on antimicrobial susceptibility testing: background, organization, functions, and processes. J Clin Microbiol. 2020;58(3):e01864-19. doi: 10.1128/jcm.01864-19.
- Pandey V, Verma RS, Chauhan A, Tiwari R. Compositional characteristics of the volatile oils of three *Artemisia* spp. from western Himalaya. J Essent Oil Res. 2015;27(2):107-14. doi: 10.1080/10412905.2014.987927.
- Chemsa AE, Zellagui A, Öztürk M, Erol E, Ceylan O, Duru ME, et al. Antibiofilm formation, antioxidant and anticholinesterase activities of essential oil and methanol extract of *Marrubium* deserti de Noé. J Mater Environ Sci. 2016;7(3):993-1000.
- Abdullah, Asghar A, Butt MS, Shahid M, Huang Q. Evaluating the antimicrobial potential of green cardamom essential oil focusing on quorum sensing inhibition of *Chromobacterium violaceum*. J Food Sci Technol. 2017;54(8):2306-15. doi: 10.1007/s13197-017-2668-7.

- 21. Rivas da Silva AC, Lopes PM, Barros de Azevedo MM, Costa DC, Alviano CS, Alviano DS. Biological activities of α -pinene and β-pinene enantiomers. Molecules. 2012;17(6):6305-16. doi: 10.3390/molecules17066305.
- 22. Julaeha E, Herlina T, Nurzaman M, Mayanti T, Kurnia D, Sari EF. The antibacterial effect of β-pinene derived from Citrus aurantifolia peel against oral Streptococcus mutans ATCC 25175. Padjadjaran J Dent. 2021;33(1):88-93. doi: 10.24198/ pjd.vol33no1.29200.
- Mostafa NM. Antibacterial activity of ginger (Zingiber officinale) leaves essential oil nanoemulsion against the cariogenic Streptococcus mutans. J Appl Pharm Sci. 2018;8(9):34-41. doi: 10.7324/japs.2018.8906.
- 24. Zare-Zardini H, Alizadeh A, Saberian E, Jenča A, Jenca A, Petrášová A, et al. Enhanced antimicrobial efficacy and biocompatibility of albumin nanoparticles loaded with Mentha extract against methicillin resistant Staphylococcus aureus. Sci Rep. 2025;15(1):6548. doi: 10.1038/s41598-025-90825-3.
- 25. Kifle D, Bacha K, Gonfa G. Antimicrobial activities of biosynthesized nanosilver using Musa paradisiaca and Citrus sinensis peel extracts against major human and plant pathogens. Sci Rep. 2025;15(1):6600. doi: 10.1038/s41598-025-91020-0.
- 26. Costa E, Silva S, Tavaria F, Pintado M. Antimicrobial and antibiofilm activity of chitosan on the oral pathogen Candida albicans. Pathogens. 2014;3(4):908-19. doi: 10.3390/ pathogens3040908.
- 27. Lo WH, Deng FS, Chang CJ, Lin CH. Synergistic antifungal activity of chitosan with fluconazole against Candida albicans, Candida tropicalis, and fluconazole-resistant strains. Molecules. 2020;25(21):5114. doi: 10.3390/ molecules25215114.
- 28. Sepahi S, Ghorani-Azam A, Sepahi S, Asoodeh A, Rostami S. In vitro study to evaluate antibacterial and non-haemolytic activities of four Iranian medicinal plants. West Indian Med J. 2014;63(4):289-93. doi: 10.7727/wimj.2013.095.
- 29. Nazemisalman B, Vahabi S, Yazdinejad A, Haghghi F, Shabbuii Jam M, Heydari F. Comparison of antimicrobial

- effect of Ziziphora tenuior, Dracocephalum moldavica, Ferula gummosa, and Prangos ferulacea essential oil with chlorhexidine on Enterococcus faecalis: an in vitro study. Dent Res J (Isfahan). 2018;15(2):111-6.
- 30. Najaf Najafi M, Arianmehr A, Sani AM. Preparation of Barije (Ferula gummosa) essential oil-loaded liposomes and evaluation of physical and antibacterial effect on Escherichia coli O157:H7. J Food Prot. 2020;83(3):511-7. doi: 10.4315/0362-028x.Jfp-19-285.
- 31. Kamelnia E, Divsalar A, Darroudi M, Yaghmaei P, Sadri K. Production of new cellulose nanocrystals from Ferula gummosa and their use in medical applications via investigation of their biodistribution. Ind Crops Prod. 2019;139:111538. doi: 10.1016/j.indcrop.2019.111538.
- 32. Mousavi-Kouhi SM, Beyk-Khormizi A, Amiri MS, Mashreghi M, Hashemzadeh A, Mohammadzadeh V, et al. Plant gelmediated synthesis of gold-coated nanoceria using Ferula gummosa: characterization and estimation of its cellular toxicity toward breast cancer cell lines. J Funct Biomater. 2023;14(7):332. doi: 10.3390/jfb14070332.
- 33. Hosseini A, Bakhtiari E, Khajavi Rad A, Shahraki S, Mousavi SH, Havakhah S, et al. The evaluation and comparing of cytotoxic effects of Ferula gummosa gum, Scutellaria lindbergii, Kelussia odoratissima and Artemisia kopetdaghensis extracts on ACHN cell line. Iran J Pharm Res. 2017;16(3):1104-12.
- 34. Forouzmand SH, Mousavi SH, Vazifedan V, Nourbakhsh M, Chamani J, Hoseini A, et al. Synergistic effects of Ferula gummosa and radiotherapy on induction of cytotoxicity in HeLa cell line. Avicenna J Phytomed. 2018;8(5):439-77.
- 35. Heydari-Majd M, Rezaeinia H, Shadan MR, Ghorani B, Tucker N. Enrichment of zein nanofibre assemblies for therapeutic delivery of Barije (Ferula gummosa Boiss) essential oil. J Drug Deliv Sci Technol. 2019;54:101290. doi: 10.1016/j. jddst.2019.101290.
- Jalili-Nik M, Soukhtanloo M, Javanshir S, Jahani Yazdi A, Esmaeilizadeh M, Jafarian AH, et al. Effects of ethanolic extract of Ferula gummosa oleo-resin in a rat model of streptozotocininduced diabetes. Res Pharm Sci. 2019;14(2):138-45. doi: 10.4103/1735-5362.253361.